ELSEVIER

Journal of Power Sources 68 (1997) 540–544

JOURNAL OF POWER SOURCES

Electrochemical characterization of thin-film $LiCoO_2$ electrodes in propylene carbonate solutions

Hajime Sato, Daisuke Takahashi, Tatsuo Nishina *, Isamu Uchida

Department of Applied Chemistry, Graduate School of Engineering, Tohoku University, Aramaki-Aoba, Aoba-Ku, Sendai 980-77, Japan

Received 28 September 1996

Abstract

Thin films of $LiCoO_2$ (0.22–1.15 μm) were prepared by oxidation of metallic cobalt in molten alkali carbonates containing Li^+ ions. We report here the behavior of the thin film of $LiCoO_2$ by cyclic voltammetry in propylene carbonate solvent systems, the kinetic analysis using electrochemical impedance spectroscopy (EIS), and potential step chronoamperometry (PSCA). The chemical diffusion coefficients for Li^+ ions in the $LiCoO_2$ electrodes were determined; $\tilde{D} = (2.3\text{–}9.0) \times 10^{-12}$ cm^2/s by PSCA, and $\tilde{D} = 0.9 \times 10^{-9}$–$2 \times 10^{-8}$ cm^2/s by EIS.

Keywords: Lithium batteries; Cobalt; Thin films; Diffusion coefficient; Electrochemical impedance spectroscopy; Lithium-ion extraction/insertion

1. Introduction

$LiCoO_2$ is currently used as a cathode material in lithium secondary batteries in commercial products [1]. For high-power applications, the Li^+ ion diffusion inside the solid must be high. However, kinetic studies on Li^+ insertion/extraction processes in $LiCoO_2$ are quite limited [2–4]. This may be due to the difficulties to analyze reliable kinetic information from the data obtained from composite-type electrodes with porous structures. In a previous paper [5], we reported the electrochemical behavior of thin $LiCoO_2$ films using cyclic voltammetry (CV) in propylene carbonate (PC) solutions. In this paper the extended analyses of the kinetic behavior using electrochemical impedance spectroscopy (EIS) and potential step chronoamperometry (PSCA) are discussed.

2. Experimental

Thin films of $LiCoO_2$ (0.22–1.15 μm) were prepared on a gold substrate (0.39 cm^2 area) by oxidation of thin cobalt films in molten Li + K carbonates (62 + 38) mol% at 923 K under an O_2/CO_2 (9:1) atmosphere [6]. The film thickness was determined by Auger electron spectroscopy and measurements of the film weight, where the value of 5.05 g cm^{-3} was used for the density of $LiCoO_2$. Electrochemical measurements were carried out with a three-electrode cell assembled in an argon-filled dry box. The electrolyte was 1 M $LiClO_4$ in PC. The reference and counter electrodes consisted of lithium foils pressed onto nickel mesh current collectors. Cyclic voltammograms (CVs) were obtained with a Princeton Applied Research (PAR) Model 273 potentiostat; EIS measurements were carried out with an electrochemical interface Solartron 1286, linked to a Solartron frequency response analyzer 1250.

3. Results and discussion

3.1. Cyclic voltammetry

The insertion/extraction behavior of Li^+ ions of an $LiCoO_2$ film (0.22 μm thickness) was characterized by CV as shown in Fig. 1. Three sets of well-defined current peaks were observed when the scan rate was lower than 1 mV/s [5]. These peaks agreed well with the $-dx/dV$ behavior reported in Ref. [7]. Since the peak current i_p of the main peak ($E_p = 3.93$ V) was proportional to the square root of the scan rate v when v was greater than 1 mV/s (Fig. 2) it may be possible to obtain the averaged chemical diffusion coefficients $\tilde{D}$ of Li^+ in the solid phase by the following equation [8]

$$i_p = 0.4463nFAC\tilde{D}^{1/2}(nF/RT)^{1/2}v^{1/2} \quad (1)$$

* Corresponding author.

0378-7753/97/$17.00
PII S0378-7753(96)02589-X

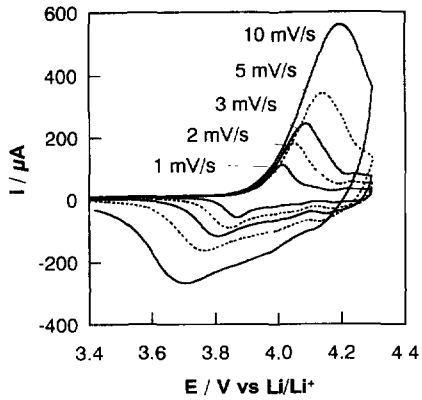

Fig. 1. Scan rate dependence of cyclic voltammograms for $LiCoO_2$ (0.22 μm) in 1 M $LiClO_4$/PC.

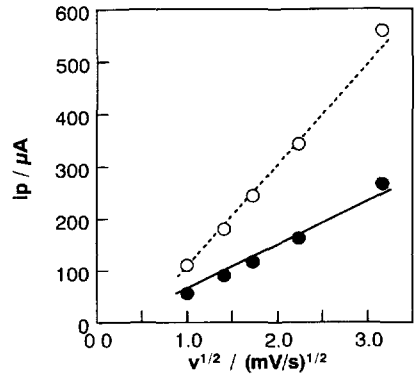

Fig. 2 Scan rate dependence of the peak current i_p for $LiCoO_2$ (0.22 μm) in 1 M $LiClO_4$/PC: (○) anodic scan peak, and (●) cathodic scan peak

Table 1
Chemical diffusion coefficient of Li^+ in $LiCoO_2$ obtained by different transient methods

Method	$\tilde{D}$ (cm^2/s)	Equation used
CV	$(0.3–9.9)\times10^{-12}$	(1)
EIS	$(0.9–20)\times10^{-9}$	(4)
PSCA	$(2.3–9.0)\times10^{-12}$	(5)
	5.0×10^{-14}	(6)

Based on the $i_p - v^{1/2}$ relation obtained in Fig. 2, the $\tilde{D}$ values were determined and the results are shown in Table 1.

3.2. Electrochemical impedance spectroscopy

Fig. 3 shows the Cole–Cole plots of the EIS spectra for a thin $LiCoO_2$ film (0.82 μm in thickness). Prior to the EIS measurements, the electrode was pretreated by a potential cycling between an open-circuit voltage (3.0 V) and 4.0 V to check the initial response of the electrode, then the EIS measurements were carried out at fixed potentials from 3.6 to 4.0 V in 50 mV intervals. At each potential, we monitored the d.c. current response to ensure that the $LiCoO_2$ electrode reached equilibrium at a given potential prior to the EIS measurements. The EIS spectra showed similar responses peculiar to thin-film electrodes as schematically shown in

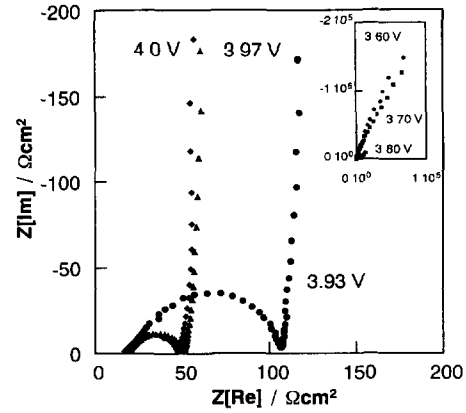

Fig. 3 Cole–Cole plots of $LiCoO_2$ (0.82 μm) obtained at different potentials (indicated in the figure) in 1 M $LiClO_4$/PC; f = 10 kHz–1 mHz.

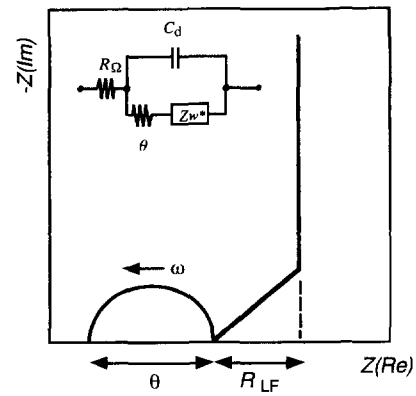

Fig. 4. Schematical setup of the complex impedance of the Randles equivalent circuit. R_Ω: solution resistance; θ: resistance of the thin-film electrode; C_d: double-layer capacitance, and Z_w*: Warburg impedance of the finite diffusion inside the film.

Fig. 4. However, we could not find any response due to the semi-infinite diffusion (Warburg impedance), which usually shows up as a 45° linear locus in the Cole–Cole plot. At lower potentials (3.6–3.8 V), only the imaginary part of the EIS increased with decreasing frequency, which is due to the capacitive response. At a higher potential range (3.8–3.95 V), a semicircular arc appeared in the high frequency range and the capacitive response was observed in the lower frequency range. The absolute values of impedance drastically decreased with increasing potential in this potential range, and subsequently they were saturated to show almost the same values at 3.95–4.0 V.

These characteristics become clear, if we plot the EIS data in a Bode-type plot as shown in Figs. 5 and 6. Fig. 5 shows the Bode plots of the real part of the EIS ($Z_{[Re]}$). $Z_{[Re]}$ values (about 20 Ω cm^2) at the high frequency end agreed well each other for all cases. That means the solution resistance. However, the plateau in the low frequency range, which corresponds to the closed end of the semicircular arc at low frequencies in Fig. 3, drastically decreased by about two orders of magnitude with increasing potential and became saturated at potentials greater than 3.95 V. The difference between the plateaus at low frequencies and at the high fre-

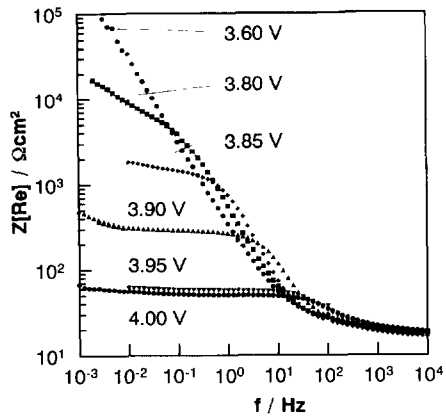

Fig. 5. Frequency dependence of impedance (real part) of $LiCoO_2$ (0.82 μm) obtained at different potentials (indicated in the figure) in 1 M $LiClO_4$/PC.

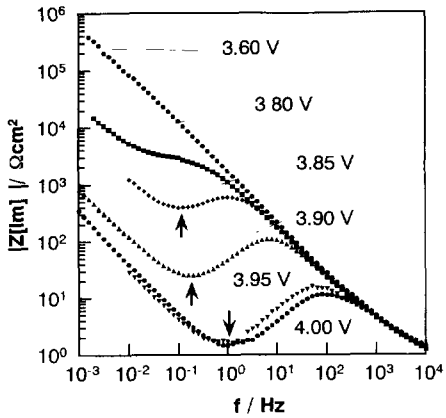

Fig. 6. Frequency dependence of impedance (imaginary part) of $LiCoO_2$ (0.82 μm) obtained at different potentials (indicated in figure) in 1 M $LiClO_4$/PC. The arrows indicate the ω_T used for calculation of diffusion coefficient.

quency end corresponds to the diameter of the semicircular arc ascribed to the resistance of the $LiCoO_2$ film. Clearly, the conductivity of $LiCoO_2$ increases with extracting Li^+ ions. Similar behavior was also seen in the Bode plots of the imaginary part of the EIS ($Z_{[Im]}$) in Fig. 6, where the peak values correspond to the radius of the semicircular arcs in Fig. 3. Apparently, the conductivity of $LiCoO_2$ increases by two orders of magnitude with extracting Li^+ ions. This result that the conductivity of $LiCoO_2$ increases with extracting Li^+ ions and it becomes saturated at potentials more positive than 3.95 V, was confirmed by our in situ conductivity measurements described elsewhere [9].

According to Ho et al. [10], the EIS spectra of the insertion/extraction reaction of Li^+ at the thin-film electrode can be expressed by the equivalent circuit as shown in Fig. 4 where R_Ω is the solution resistance, θ the resistance of the thin-film electrode, C_d the double-layer capacitance and Z_w* the Warburg impedance of the finite diffusion inside the film. Z_w* comprises two regions: (i) the semi-infinite diffusion case in a high frequency range where the penetration depth of the concentration wave is smaller than the film thickness, h, and (ii) the finite diffusion case in a lower frequency range where the concentration wave reaches the film thickness.

(i) Semi-infinite diffusion case

$$Z_w^* = (1-j)\frac{V_M(dE/dy)}{\sqrt{2}zFA\sqrt{\tilde{D}}}\omega^{1/2} \quad \text{for } \omega \gg 2\tilde{D}/h^2 \tag{2}$$

(ii) Finite diffusion case

$$Z_w^* = R_{LF} - j\frac{1}{\omega C_{LF}} = \frac{V_M(dE/dy)}{zFA}\frac{h}{3D} - j\frac{V_M(dE/dy)}{zFAh}\frac{1}{\omega} \quad \text{for } \omega \ll 2\tilde{D}/h^2 \tag{3}$$

where V_M is the molecular volume, $\tilde{D}$ the chemical diffusion coefficient, z the valence of the diffusing ion, A the electrode surface area, and y the mole fraction of the diffusing ion in the film. R_{LF} can be determined by using semi-infinite diffusion as shown in Fig. 4, and C_{LF} can be obtained directly from the imaginary part of the impedance in the finite diffusion range. By equating Eqs. (2) and (3), the transition angular velocity, ω_T, which is the point at which the transition from semi-infinite diffusion to finite diffusion occurs, is obtained as follows

$$\omega_T = \frac{2\tilde{D}}{h^2} \tag{4}$$

Thus, $\tilde{D}$ can be determined from R_{LF} and C_{LF} using Eq. (3), or from ω_T values using Eq. (4), if the film thickness h is known.

Unfortunately, it is impossible to apply this technique to the present response of thin-film $LiCoO_2$ electrodes, because we could not observe any semi-infinite diffusion response in the EIS spectra as demonstrated in Fig. 3. This may be attributed to the small value of dE/dy and large value of θ. The small value of dE/dy makes R_{LF} very small and it may be hindered by the large θ. However, it may be possible to estimate the $\tilde{D}$ values if we can estimate ω_T. As shown in Fig. 6, the imaginary part of the impedance in the low frequency range decreased rapidly with increasing frequency and reached a minimum value as indicated by arrows. Since the linearity of the log–log plots at the low frequency range was fairly good and the R_{LF} values seemed to be very small, the angular velocity at this minimum point can be regarded as a good approximation of ω_T. Therefore, we calculated the $\tilde{D}$ values from the angular velocity at this minimum point by using Eq. (4). The $\tilde{D}$ values determined are summarized in Fig. 7 as a function of potential and in Table 1. As shown in Fig. 7, $\tilde{D}$ values showed $(0.9–20) \times 10^{-9}$ cm^2/s, dependent on the potential and seemed to reach a maximum in the positive potential 3.95–4.0 V range.

3.3. Potential step chronoamperometry

Current responses to a potential step are shown in Fig. 8. In order to analyze these data we used the equation derived

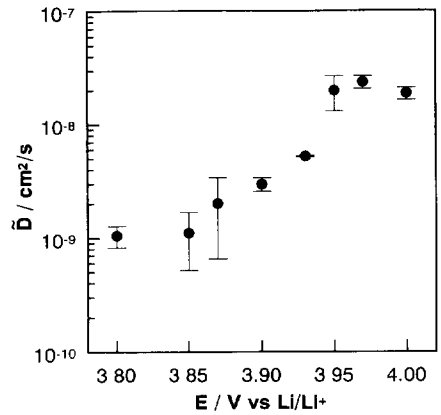

Fig. 7 Diffusion coefficients as a function of electrode potential, calculated from EIS method.

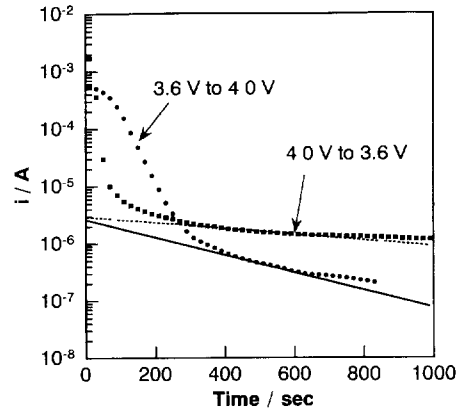

Fig. 8. Cathodic and anodic current decays for $LiCoO_2$ (0.82 μm) in 1 M $LiClO_4$/PC. The stepped potentials from the initial are indicated in figure Solid line and dotted line are theoretical based on Eq (5).

by MacArthur [11] for the determination of diffusion coefficient

$$\ln|i_{diff}| = \ln\left|\frac{n_e FA\tilde{D}2C}{h}\right| - \frac{\tilde{D}\pi^2}{4h^2}t \qquad (5)$$

Eq. (5) can be applied to data obtained for long time periods, i.e. 400–800 s. Based on Eq. (5), we plotted log i against t, and obtained the $\tilde{D}$ values from the slope and the intersection.

Rajan and Neff [12] proposed a new treatment taking into account the charge migration caused by a potential gradient within a film. For an oxidation pulse

$$i = \frac{2n_0 F\tilde{D}}{h^2}\exp\left\{-\frac{\tilde{D}}{h^2}\left[\frac{\pi^2}{4} + \frac{F\Delta\Psi}{RT}\left(\frac{F\Delta\Psi}{4RT}+1\right)\right]t\right\} \qquad (6)$$

where n_0 is the initial number of moles of Li^+ ion in $LiCoO_2$, and $\Delta\Psi$ is a potential difference within the film generated by the external potential step. The second term within the brackets expresses the effect of the migration of Li^+ ions in the solid phase driven by $\Delta\Psi$. If $\Delta\Psi$ is close to zero, this equation is equal to MacArthur's equation. We used the relation between log i and t to obtain $\tilde{D}$ values by both MacArthur's method and Neff's method. The results are compared in Table 1.

The determined $\tilde{D}$ values are summarized in Table 1. In EIS measurements, the $\tilde{D}$ values were obtained as a function of the electrode potential, while the other methods gave apparent values averaged over the potential dependence. It is noted that the EIS method gives considerably higher $\tilde{D}$ values (10^{-9}–10^{-8} cm^2/s) than those ($\sim 10^{-12}$ cm^2/s) by the transient methods. Further studies are needed to clarify which method can give resonable $\tilde{D}$ values.

A comparison of the $\tilde{D}$ values with data found in the literature is summarized in Table 2. Present results showed lower values than those reported in the literature [2–4]. In this work, binder-free, thin-film electrodes were used, whereas methods given in the literature employed composite-type electrodes with relatively thick sheets or pellets. Generally speaking, the thin-film experiment tends to give the lower values ($\sim 10^{-12}$ cm^2/s) of $\tilde{D}$ than the sheet-type experiments even for other oxides, e.g., $(2.4\text{–}28)\times 10^{-12}$ cm^2/s for vapor-deposited Li_xWO_3 thin films [10] and $(0.58\text{–}5)\times 10^{-12}$ cm^2/s for CVD-formed Li_xMoS_2 thin films [13].

The great $\tilde{D}$ values observed in the composite electrodes can be attributed to the nature of the porous electrodes; high surface area; increased ionic conductivity due to the impregnated electrolyte, and high rates of ion transport through the interface between the dispersed particles and the electrolyte channels. Inside the porous composite body, the dispersed particles may act as single electrodes with μm sizes, nevertheless the $\tilde{D}$ values are determined by using the overall

Table 2
The chemical diffusion coefficient of Li^+ ions in Li_xCoO_2

	Method	Electrolyte	Electrode size	x value in Li_xCoO_2	$\tilde{D}$ (cm^2/s)
This work	PSCA	1 M $LiClO_4$/PC	Diameter: 5 mm, h = 0.82 μm	$0.7 < x < 1.0$	$(2.3\text{–}9)\times 10^{-12}$
This work	EIS	1 M $LiClO_4$/PC	Diameter: 5 mm, h = 0.82 μm	$0.7 < x < 1.0$	$(0.9\text{–}20)\times 10^{-9}$
Ref [2]	GITT [a]	1 M $LiBF_4$/PC	Diameter: 10 mm	$0.2 < x < 0.8$	5×10^{-9}
Ref. [3]	Potential step and current pulse/ voltage decay	1 M $LiClO_4$/PC	Diameter: 8 mm, h = 0.18 mm	$0.1 < x < 1.0$	$(2\text{–}40)\times 10^{-9}$
Ref. [4]	EIS	1 M $LiBF_4$/PC	Diameter: 13 mm	$0.2 < x < 0.55$	$(5\text{–}7)\times 10^{-8}$

[a] Galvanostatic intermittent titration technique

thickness of the sheet/pellet)-type electrode. This may cause a significantly large $\tilde{D}$ value.

Acknowledgements

This research was supported by Grand-in-Aid for Scientific Research (No. 06 453 111) of The Ministry of Education, Science and Culture.

References

[1] K. Ozawa, *Solid State Ionics, 69* (1994) 212
[2] K. Mizushima, P.C. Jones, P.J. Wiseman and J.B. Goodenough, *Solid State Ionics, 3/4* (1981) 171.
[3] A. Honders, J.M. der Kinderen, A.H. van Heeren, J.H.W. de Wit and G.H.J. Broers, *Solid State Ionics, 15* (1985) 265.
[4] M.G.S.R. Thomas, P.G. Bruce and J.B. Goodenough, *Solid State Ionics, 17* (1985) 13.
[5] I. Uchida and H. Sato, *J. Electrochem. Soc., 142* (1995) L139.
[6] K. Yamada and I. Uchida, *Chem. Lett.*, (1994) 299.
[7] J.N. Reimers and J R Dahn, *J. Electrochem Soc., 139* (1992) 2091.
[8] A.J. Bard and L.R. Faulkner, *Electrochemical Methods*, Wiley, New York, 1980, p. 218.
[9] M. Shibuya, S. Yamamura, S. Waki, T. Matue and I. Uchida, *J. Electrochem. Soc., 143* (1996) 3154.
[10] C. Ho, I.D. Raistrick and R.A. Huggins, *J. Electrochem. Soc., 127* (1980) 343.
[11] D.M. MacArthur, *J. Electrochem Soc., 117* (1970) 729.
[12] K.P. Rajan and V.D. Neff, *J. Phys. Chem., 86* (1982) 4361.
[13] N. Imanishi, K. Kanamura and Z.-i. Takehara, *J. Electrochem. Soc., 139* (1992) 2082.